

Investigation of whispering gallery mode dependence on cavity geometry of quasiperiodic photonic crystal microcavity lasers

Po-Tsung Lee, Tsan-Wen Lu, Feng-Mao Tsai, and Tien-Chang Lu

Citation: *Applied Physics Letters* **89**, 231111 (2006); doi: 10.1063/1.2402894

View online: <http://dx.doi.org/10.1063/1.2402894>

View Table of Contents: <http://scitation.aip.org/content/aip/journal/apl/89/23?ver=pdfcov>

Published by the [AIP Publishing](#)

Articles you may be interested in

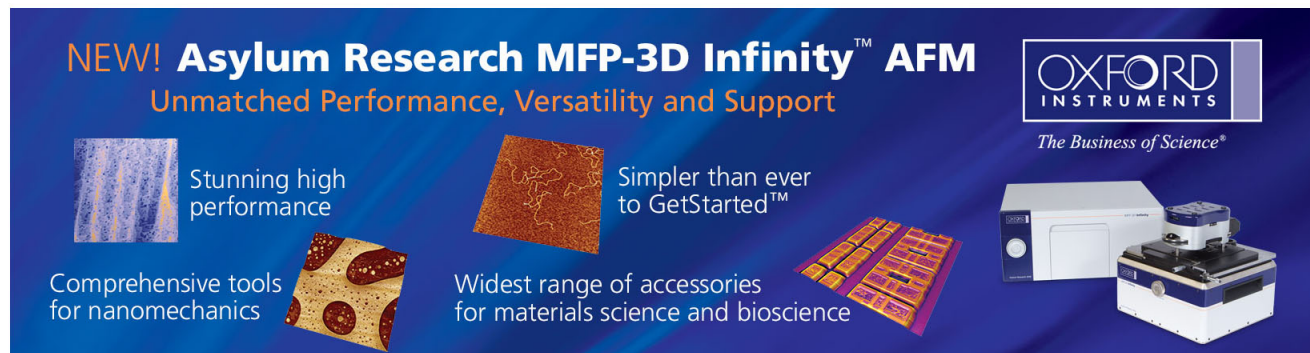
[Exciton-polariton microphotoluminescence and lasing from ZnO whispering-gallery mode microcavities](#)
Appl. Phys. Lett. **98**, 161110 (2011); 10.1063/1.3579140

[Combined whispering gallery mode laser from hexagonal ZnO microcavities](#)
Appl. Phys. Lett. **95**, 191117 (2009); 10.1063/1.3264080

[Whispering gallery modes in hollow cylindrical microcavities containing silicon nanocrystals](#)
Appl. Phys. Lett. **92**, 131119 (2008); 10.1063/1.2903134

[High quality factor microcavity lasers realized by circular photonic crystal with isotropic photonic band gap effect](#)
Appl. Phys. Lett. **90**, 151125 (2007); 10.1063/1.2724899

[Whispering gallery mode of modified octagonal quasiperiodic photonic crystal single-defect microcavity and its side-mode reduction](#)
Appl. Phys. Lett. **88**, 201104 (2006); 10.1063/1.2203943

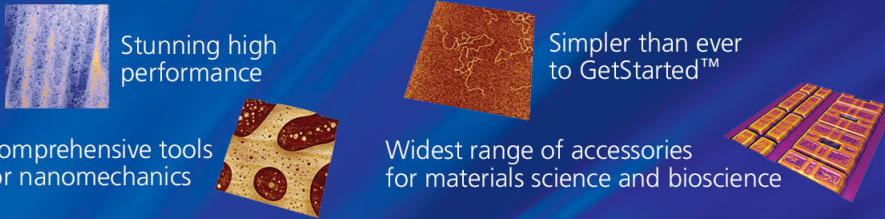


NEW! Asylum Research MFP-3D Infinity™ AFM
Unmatched Performance, Versatility and Support

OXFORD INSTRUMENTS
The Business of Science®

Stunning high performance
Simpler than ever to GetStarted™

Comprehensive tools for nanomechanics
Widest range of accessories for materials science and bioscience



Investigation of whispering gallery mode dependence on cavity geometry of quasiperiodic photonic crystal microcavity lasers

Po-Tsung Lee, Tsan-Wen Lu,^{a)} Feng-Mao Tsai, and Tien-Chang Lu

Department of Photonics and Institute of Electro-Optical Engineering, National Chiao Tung University, Rm. 415, CPT Building, 1001 Ta-Hsueh Road, Hsinchu, 300 Taiwan, Republic of China

(Received 1 August 2006; accepted 26 October 2006; published online 6 December 2006)

Dodecagonal (12-fold) quasiperiodic photonic crystal (DQPC) microcavity lasers sustaining whispering gallery mode (WGM) are fabricated. Lasing characteristics of DQPC D2 microcavity lasers are obtained and compared with triangular lattice D2 photonic crystal (PC) lasers, and ultralow threshold is obtained. The strong WGM mode dependence on 12 nearest airholes of DQPC D2 microcavity and its fabrication tolerance is investigated and discussed by randomly varying the lattice of two separate regions. This mode dependence also indicates that one can enhance a WGM in different PC microcavities by modifying the cavity boundary to be circular. © 2006 American Institute of Physics. [DOI: 10.1063/1.2402894]

Since photonic crystal (PC) microcavity laser was first demonstrated by Painter *et al.*,¹ various attractive PC microcavities with different lattices, cavity geometries, and device structures have been widely investigated.^{2–5} With photonic band-gap (PBG) effect, the well-controlled photon flows in PC microcavities are extremely potential for quantum-electron dynamics devices and integrated photonic applications due to its ultrahigh quality (Q) factor and ultralow threshold. However, the anisotropy of PBG caused by the low-level symmetry in wave-vector (k) space has been found and investigated.^{6,7} Actually, higher-level symmetry can be obtained by applying quasiperiodic lattice originated from solid-state physics and the anisotropy of PBG can be reduced. PC microcavities with different quasiperiodic lattices have been investigated in theory by several groups.^{8–10} As the mirror of microcavity, quasiperiodic photonic crystal (QPC) would provide more efficient and uniform in-plane confinement in all directions,¹¹ which is beneficial to achieving lasing properties of lower threshold and higher Q factor. Besides, with proper design, whispering gallery mode (WGM) with high Q factor can be sustained in a two-dimensional QPC microcavity, which is confined in-plane by both the PBG effect and total internal reflection effect. However, up to date, only a few groups, for example, Nozaki and Baba⁸ and Kim *et al.*,¹⁰ make efforts on the study of localized states in dodecagonal (12-fold) QPC (DQPC) microcavities in experiments. In this letter, we design and fabricate DQPC microcavity lasers formed by seven missing airholes (D2) using finite-difference time-domain (FDTD) method and a series of dry/wet etching processes. We obtain the lasing characteristics of DQPC D2 microcavities and compared them with triangular lattice PC lasers with similar cavity sizes. We also investigate the strong WGM mode dependence on the 12 nearest airholes and the tolerance of fabrication imperfection in DQPC microcavity lasers from statistical measurement results by randomly varying the positions of 12 nearest or outer airholes.

At first, we calculate the profiles of resonance modes in the DQPC D2 microcavity using two-dimensional (2D) FDTD method with an approximated index of 2.7. One cal-

culated mode presents zero-order radial WGM profile with azimuthal number 6 (W6 mode), as shown in Fig. 1(a), which agrees with the results in Ref. 9. W6 mode is a very potential mode due to its high Q factor [over 200 000 (Ref. 12)] contributed to the good consistency with cavity geometry. More important, its central node with zero field distribution is quite suitable for electrical injection structure used in microdisk lasers. In Fig. 1(a), we also show the other two zero-order radial modes with azimuthal numbers 5 (W5 mode) and 4 (W4 mode) and a first-order radial mode with azimuthal number 3 (W3 mode), which are with lower Q factors and near the W6 mode in spectrum. In this report, we will focus on the W6 mode. More details of simulation parameters and related simulations can be found in recent reports by our group¹³ and Nozaki *et al.*⁸

In fabrication, at first, the epitaxial structure consisting of four 10 nm compressively strained InGaAsP multi-quantum-wells (MQWs) on InP substrate as the active layer with 1550 nm central wavelength under photoluminescence (PL) is prepared. Then we deposit Si_3N_4 layer as an etching mask by plasma enhanced chemical vapor deposition process. A polymethylmethacrylate electron-beam resist layer is

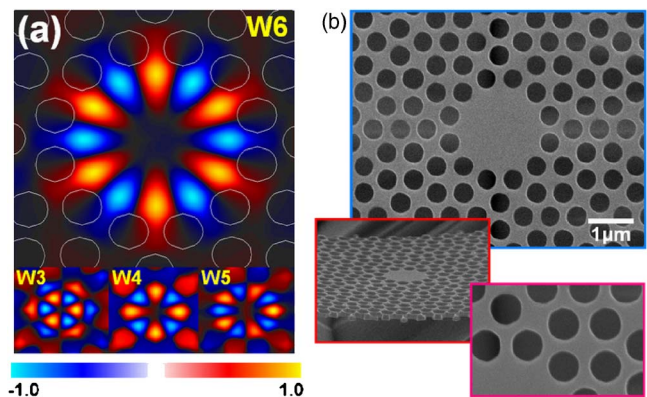


FIG. 1. (Color online) (a) Main resonance mode, WGM, with azimuthal number 6 (W6 mode) is calculated by 2D FDTD method. Other resonance modes (W3, W4, and W5) near the W6 mode in spectrum are also calculated. (b) Top view and tilted view SEM pictures of a typical DQPC D2 microcavity. The fabricated lattice constant and airhole radius are 600 and 220 nm.

^{a)}FAX: 886-3-5735601; electronic mail: ricky.eo94g@nctu.edu.tw

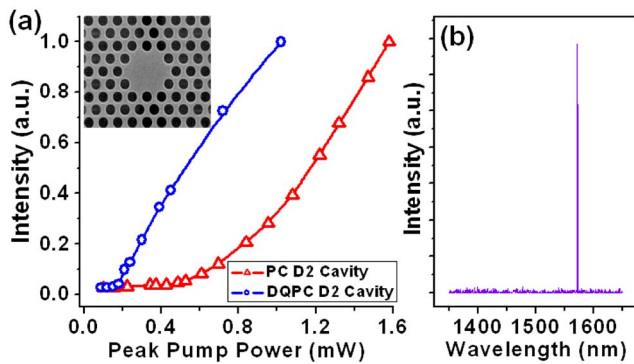


FIG. 2. (Color online) (a) Typical L-L curves of DQPC and triangular PC D2 microcavity lasers. The thresholds of DQPC and PC D2 lasers can be estimated as 0.15 and 0.6 mW at similar lasing wavelengths. (b) Typical lasing spectrum of DQPC D2 microcavity laser. The lasing wavelength is 1572 nm and its FWHM is 0.15 nm.

spun on Si_3N_4 layer, and the DQPC microcavity patterns are defined by electron-beam lithography system. For transferring DQPC patterns into InGaAsP/InP layers, the inductively coupled plasma/reactive ion etching (ICP/RIE) system is used. The Si_3N_4 hard mask is etched by CHF_3/O_2 mixed gas in RIE-mode dry etching, and then $\text{CH}_4/\text{Cl}_2/\text{H}_2$ mixed gas is used to transfer the patterns into MQWs at 150 °C in ICP etching mode. Finally, a suspended membrane is formed by HCl selective wet etching. The top view and tilted view scanning electron microscope (SEM) pictures of fabricated high quality DQPC D2 microcavity are shown in Fig. 1(b). The fabricated lattice constant (a) and airhole radius (r) are 600 and 220 nm.

In the PL measurements, the microcavity is optically pulse pumped at room temperature by a laser diode of 845 nm with 25 ns pulse width and 0.5% duty cycle. Light emitted from the cavity is collected by a multimode fiber and detected by an optical spectrum analyzer. The light-in light-out curve (L-L curve) and typical lasing spectrum of DQPC D2 microcavity are shown in Figs. 2(a) and 2(b). We obtain the ultralow threshold of 0.15 mW of DQPC D2 microcavity from the L-L curve and its full width at half maximum (FWHM) is 0.15 nm at 1572 nm. We also fabricate PC D2 microcavity laser with triangular lattice by the same process and on the same wafer for comparisons. The Q factor of main lasing mode of PC D2 microcavity is about 3000–4000.¹⁴ Its L-L curve and SEM picture are shown in Fig. 2(a) and its inset. The threshold of PC D2 microcavity laser with single-mode lasing at a similar lasing wavelength is 0.6 mW and its FWHM is around 0.3 nm, which both indicate the better performance of DQPC lasers resulted from the more uniform and efficient confinement provided by DQPC and the presence of WGM. Besides, this threshold of 0.15 mW is also lower than the 0.3 mW of the single-defect microcavity laser with lower symmetry (eightfold) QPCs in our previous work.¹³

In Fig. 1(a), the W6 mode profile has good consistency with the gears formed by the 12 nearest airholes surrounding the cavity. This also implies the strong mode dependence of W6 mode on the positions of 12 nearest airholes. To obtain more direct evidence supporting this assumption, we randomly vary the positions of the 12 nearest airholes (denoted by red circles, region A) and the outer airholes (denoted by blue circles, region B) separately, as shown in Fig. 3(a). The degrees of variation are from 1% to 7% of lattice constant

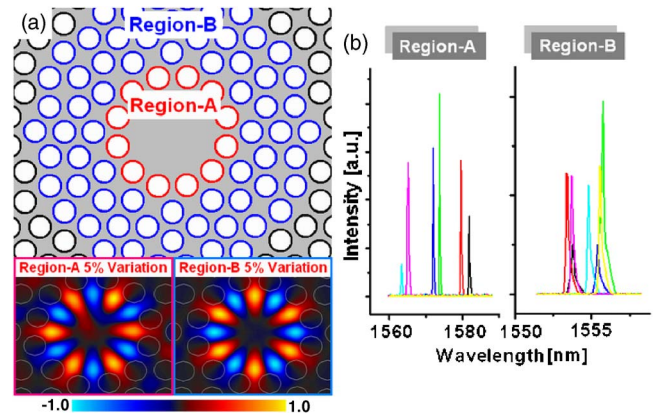


FIG. 3. (Color online) (a) Illustration of two variation regions, the 12 nearest airholes (denoted by red circles, region A) and the outer airholes (denoted by blue circles, region B) in DQPC D2 microcavity. The mode distortions of these two cases with the same variation degree of 5% are also shown. (b) Lasing spectra of devices with different variation degrees in regions A and B. Lasing wavelength variations for the region-A and -B cases are 19 and 2.5 nm.

with fixed r/a ratio and lattice constant. Lasing spectra of devices with randomly varying the airhole positions in regions A and B are shown in Fig. 3(b). The wavelength fluctuations for the region-A and -B cases are 19 and 2.5 nm, respectively. In the region-A case, when 12 nearest airhole positions are randomly shifted, the original W6 mode tends to self-optimize its resonance behavior according to this fluctuation and the constructive interference condition provided by the nearest air holes is degraded. However, in the region-B case, it can be treated as the modal boundary condition (positions of 12 nearest airholes) is invariant, leads to almost the same lasing wavelength and threshold. The small wavelength variation of 2.5 nm in the region-B case is caused by very slight hole-radius differences occurred during the electron-beam lithography process. Besides, the band gap shifting effect caused by the lattice fluctuation can be neglected due to the relative large band gap of DQPCs.¹⁰ In Fig. 3(a), we also show examples of mode distortions for the two cases with the same variation degree of 5%. One can see significant mode distortion for the region-A case, but not for the region-B case compared to Fig. 1(a). Thus, the lasing wavelength variation is mainly caused by randomly varying the region-A lattice, which indicates the strong mode dependency of W6 mode on the 12 nearest airholes.

The statistical measurement results of these two cases are summarized in Table I. The number of sampling devices is over 300. For the region-A case, lasing actions are not always observed with lattice variation degree of 5%. When the lattice variation degree increases up to 7%, only 40% of devices exhibit lasing actions with much higher thresholds than those without variation. However, for the region-B case, we still observe lasing actions for 90% of devices when the variation increases up to 7%. These statistical results, once

TABLE I. Observed lasing actions of DQPC D2 microcavity lasers with different variation regions and degrees. The sampling devices are over 300.

Variation	0%	1%–4%	5%	7%
Region A	100%	100%	70%	40%
Region B	100%	100%	100%	90%

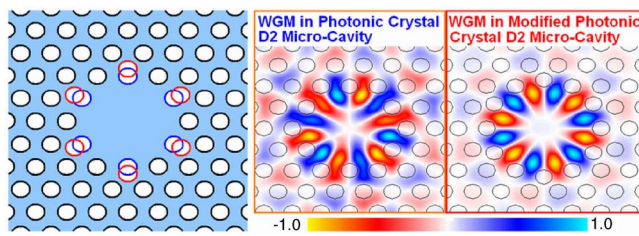


FIG. 4. (Color online) WGM in triangular PC D2 microcavity shows the mismatch between the mode profile and the cavity boundary. Well-confined WGM is sustained in modified PC D2 microcavity by shifting six nearest airholes outward to form a circular cavity boundary.

again, directly indicate the strong mode dependence of W6 mode on 12 nearest airholes. Furthermore, we also investigate the case with both region-A and -B variations. The lasing action is not always observed when the lattice variation degree is 5%. This means that the allowed variation degree is still much larger than the variation occurred in present electron-beam lithography process, which promises sufficient fabrication tolerance with constant device performance.

For past decades, WGM shows strong potential in microscale laser cavity due to its high Q factor. However, in most PC microcavities, for example, triangular PC D2 microcavity, WGM is weakly confined and exists with only several hundreds or lower Q factor due to the mismatch between cavity boundary and its mode profile. The calculated WGM profile in triangular PC D2 microcavity by FDTD method shown in Fig. 4 shows this phenomenon. As a result, the strong mode dependence on cavity boundary geometry of WGM in DQPC microcavity discussed above is quite important. It clearly indicates that one can enhance or well localize a high Q WGM in different PC microcavities by modifying only the nearest airholes of the microcavity to be a circular geometry. According to this conclusion, we shift the positions of six nearest airholes at cavity boundary denoted by blue circles outward to the positions denoted by red circles, as shown in Fig. 4 for a triangular PC D2 microcavity. Under this modification, we successfully obtain a well-confined WGM in this microcavity with circular cavity boundary, as shown in Fig. 4.

In summary, we investigate the WGM in DQPC (12-fold) D2 microcavity by FDTD method and fabricate the real devices by a series of etching processes. We obtain much lower threshold of 0.15 mW compared to 0.6 mW of trian-

gular PC D2 microcavity at similar lasing wavelengths, which is ascribed to the better confinement provided by DQPCs and presence of WGM. We also investigate the WGM mode dependence on the cavity geometry by varying the positions of 12 nearest airholes and outer airholes separately. From statistical measurement results, we show the large fabrication imperfection tolerance up to 4%, which is much larger than the variation occurred in present electron-beam lithography process. At last, according to the strong mode dependence on the 12 nearest airholes of WGM in DQPC microcavity, we successfully enhance a well-confined WGM in triangular PC D2 microcavity by shifting the positions of nearest airholes to be circular cavity boundary.

This work is supported by Taiwan's National Science Council (NSC) under Contract Nos. NSC-95-2221-E-009-234 and NSC-95-2221-E-009-056 and Promoting Academic Excellence of Universities under Contract No. NSC-94-2752-E-009-007-PAE. The authors would like to thank the help from Hao-Chung Kuo and Center for Nano Science and Technology of National Chiao Tung University, Taiwan, R. O. C.

¹O. Painter, R. K. Lee, A. Scherer, A. Yariv, J. D. O'Brien, P. D. Dapkus, and I. Kim, *Science* **284**, 1819 (1999).

²H. Y. Ryu, J. K. Hwang, and Y. H. Lee, *IEEE J. Quantum Electron.* **39**, 314 (2003).

³Y. Akahane, T. Asano, B. S. Song, and S. Noda, *Nature (London)* **425**, 944 (2003).

⁴W. D. Zhou, J. Sabarinathan, P. Bhattacharya, B. Kochman, E. W. Berg, P. C. Yu, and S. W. Pang, *IEEE J. Quantum Electron.* **37**, 1153 (2001).

⁵H. G. Park, S. H. Kim, S. H. Kwon, Y. G. Ju, J. K. Yang, J. H. Baek, S. B. Kim, and Y. H. Lee, *Science* **305**, 1444 (2004).

⁶D. Cassagne, C. Jouanin, and D. Bertho, *Phys. Rev. B* **53**, 7134 (1996).

⁷A. Barra, D. Cassagne, and C. Jouanin, *Appl. Phys. Lett.* **72**, 627 (1998).

⁸K. Nozaki and T. Baba, *Appl. Phys. Lett.* **84**, 4875 (2004).

⁹J. Chaloupka, J. Zarbakhsh, and K. Hingerl, *Phys. Rev. B* **72**, 085122 (2005).

¹⁰S. K. Kim, J. H. Lee, S. H. Kim, I. K. Hwang, Y. H. Lee, and S. B. Kim, *Appl. Phys. Lett.* **86**, 031101 (2005).

¹¹M. E. Zoorob, M. D. B. Charlton, G. J. Parker, J. J. Baumberg, and M. C. Netti, *Nature (London)* **404**, 740 (2000).

¹²K. Nozaki, A. Nakagawa, D. Sano, and T. Baba, *IEEE J. Sel. Top. Quantum Electron.* **9**, 1355 (2003).

¹³P. T. Lee, T. W. Lu, F. M. Tsai, T. C. Lu, and H. C. Kuo, *Appl. Phys. Lett.* **88**, 201104 (2006).

¹⁴C. Reese, B. Bayral, B. D. Gerardot, A. Imamoglu, P. M. Petroff, and E. Hu, *J. Vac. Sci. Technol. B* **19**, 2749 (2001).